IJISET - International Journal of Innovative Science, Engineering & Technology, Vol. 3 Issue 7, July 2016
ISSN (Online) 2348 – 7968 | Impact Factor (2015) - 4.332
www.ijiset.com

Preparation Calcium Phosphate Bio-ceramic Powders from Rubber Wood Ash

M. Masae[1*], W. Sririkun[1], P. Kongsong[2] and A. Jeenarong[3]

[1]Department of Industrial Engineering, Faculty of Engineering, Rajamangala University of Technology Srivijaya, Songkhla 90000, Thailand

[2]Department of Materials Engineering, Faculty of Engineering and Architecture, Rajamangala University of Technology Isan, NakhonRatchasima 30000, Thailand

[3]School of Health Science, Traditional Chinese Medicine, Mae FahLuang University, Chiangrai 57100, Thailand
* Corresponding author, e-mail: susumeme1983@yahoo.com

Abstract

Rubber wood ash (RWA) a predominantly source of calcium carbonate, was used as a starting material for synthesizing hydroxyapatite (HA, $(Ca)_{10},(PO_4)_6(OH)_2$) powder. The sol–gel prepared hydroxyapatite powder was characterized for its phase purity, chemical composition. Fourier transform infrared (FTIR) spectroscopy was used to identify the functional groups. X-ray diffraction (XRD) analysis was carried out to study the phase structure, crystallinity and the crystallite size of hydroxyapatite powders that were mixed with RWA for different P_2O_5 dosages sintered at 800°C. From XRD results, HA synthesized from RWA exhibited good aspect ratios with the crystalline HA structures of natural human bone. The HA produced was of comparable quality to the standard JCPDS file no. 09-0432. Morphology of scanning electron microscopy (SEM) showed that the obtained powder after sintering at 800°C is composed of hydroxyapatite nanoparticles (50–100 nm).

Keywords: *apatite, bio-ceramics, calcium hydroxyapatite, rubber wood ash (RWA).*

1. Introduction

The calcium phosphate materials, including hydroxyapatite (HA) with the formula $Ca_{10}(PO_4)_6(OH)_2$ where the Ca/P molar ratio is 1.67. Form part of the isomorphic family of apatites. HA based ceramic materials, a widely used material of choice for many applications, HA in different physical forms finds application in tissue engineering [1], drug delivery [2], implants [3], and bones cement [4]. High stability of HA in a wide range of physical conditions makes it a desirable material for other industries. Apart from the biomedical applications, HA can be utilize as catalysis [5], in adsorption processes [6], or in chromatography [7]. In most cases its applications, hydroxyapatite has a form of nanoparticles (nHA), sometimes with different sizes and morphologies: from plates, through rod-shape nanoparticles, to spherical nanoparticles. Many processes have been used to prepare HA powders including hydrolysis of other calcium phosphates [8], hydrothermal [9], precipitation from aqueous solution [10], sol-gel procedure [11 and mechanochemical synthesis [12]. The use of conventional raw material as a hydroxyapatite like oyster shell [13], eggshells [14], animal bones [15], waste mussel shells [16] and waste fish scale [17]. Reports attempting to produce or synthesize materials with chemical characteristics and waste from animal to providing a calcium-rich source that can be used to produce calcium oxide (lime), but studies on from waste plants and their phase composition and physical properties have seldom been reported.

Rubber wood is a type of wood from the Pará rubber tree (*Hevea brasiliensis*). There are numerous plantations with these types of trees in Southeast Asia. The traditional practice to extract latex from these trees was to burn the tree. Rubber wood is used only after it completes its latex producing cycle, generally in 25-30 years old. When the latex yields become extremely low, the trees are then replaced for new ones. This latex can also be used as fuel, either in a furnace, a generator, or in a steam boiler power. The latex may also be smelted into charcoal. Rubber wood ash (RWA) is abundant among the agricultural waste. This waste accounts for the annual gross rubber wood ash, 217 million metric tons of the annual gross waste in Thailand [18]. Accordingly, the aim of the present work is to synthesis a simple method for producing HA from rubber wood ash.

2. Materials and Methods

2.1 Preparation of calcium phosphate bioceramic powders

A stoichiometric amount of calcium carbonate ($CaCO_3$) from rubber wood ash (RWA) after sintered at 800°C was collected from Yala Province, Thailand. Phosphoric pentoxide (P_2O_5, Merck) were used with the molar ratio of 10:3, 10:5 and 10:7 which is the desired Ca/P ratio observed in hydroxyapatite. Absolute ethanol (C_2H_5OH, Merck) was used as the solvent. The as prepared solution after dissolving the above precursors slowly transforms into a gel after 24 h under continuously stirring at ambient temperature. Gel was aged for 12 h, and then dried in a convectional oven at 80°C for 24 h. The dried gel was sintered at a rate of 10 °C/min up to 800°C in a furnace. At the end the gel was placed in air for cooling to ambient temperature. More ever to find the effect of sintering temperature on the crystallinity of products, sintering process was also performed at temperatures of 800°C. The schematic diagram of preparing procedures of sample was described in Fig. 1.

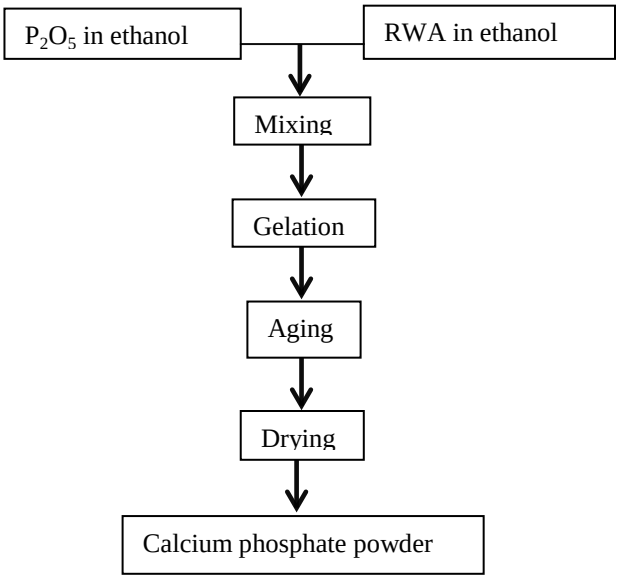

Fig. 1. Flow chart of the sol–gel synthesis of calcium phosphate powder.

2.1 Materials Characterization

The X-ray fluorescence (XRF) analysis using a Philips X'Pert MPD-PW2400 was carried out to determine chemical compositions of RWA after sintered at 800°C compared with commercial ($CaHPO_4$), calcium phosphate, (assay 98-102.5% Sigma-Aldrich, Germany). Fourier transform infrared (FTIR) spectroscopy analysis (Bruker EQUINOX 55) was carried out to identify the functional groups. The spectrum was recorded in the 4000–400 cm^{-1} region with 2 cm^{-1} resolution. The morphology of calcium phosphate powders was investigated with a scanning electron microscope (SEM; JEOL JSM- 5800LV). The phase composition analysis was carried out by X-ray diffraction (XRD) method using a Philips X'Pert-MPD System powder diffract meter with Cu Kα radiation over the 2θ range of 20–60° at a scan rate of 0.02°/min. The crystallite size was determined from XRD peaks using the Scherer equation [19],

$$d = \frac{(0.9\lambda)}{(FWHMCOS\theta)} \quad \text{..... (1)}$$

Where d is crystallite size, λ is the wavelength of the X-ray radiation (Cu-Kα = 0.15406 nm), FWHM the full width at half maximum for the diffraction peak under consideration (rad), and θ is the diffraction angle (°).

The fraction of crystalline phase (F_c) in the hydroxyapatite powders can be evaluated by the following equation (2) [20]:

$$F_c = 1 - \frac{V_{112/300}}{I_{300}} \quad \text{..... ..... (2)}$$

where I_{300} is the intensity of (300) diffraction peak and $V_{112/300}$ is the intensity of the hollow between (112) and (300) diffraction peaks of hydroxyapatite.

3. Results and Discussion

Chemical composition of RWA is 48.24% CaO was found to be the main content in RWA similar with the commercial calcium phosphate (Table 1). Fig. 2 shows the XRD patterns of RWA after sintered at 800°C was presented. The RWA patterns were identified as JCPDS (HA) the file No. 09-0432 compared with commercial calcium phosphate ($CaHPO_4$). The XRD patterns of prepared hydroxyapatite powders at different amount of P_2O_5 are also shown in Fig. 3. Broad diffraction peaks of all samples can be observed. Crystalline hydroxyapatite starts to form due to sintering process at 800°C. Amount of P_2O_5 plays an important role on the formation of hydroxyapatite (Fig. 3.). As the amount of P_2O_5 is increased from 3 to 7, several peaks of the hydroxyapatite become more distinct and also the widths of the peaks become narrower, which suggests an increase in the degree of crystallinity. It can also be seen additional crystalline phases β-TCP ($Ca_3(PO_4)_2$) appear in a small trace from the original calcination process since the transformation of the raw RWA to lime is between 81-87% as shown in Table 2. The XRD patterns for RWA powders after sintered at 800 °C appear very similar to those that show

signature peaks for HA (JCPDS 09-0432), as shown in the curves labeled a and c in Fig. 2. The peaks obtained from the powder after calcination at 800 °C becomes significantly sharper, revealing pure crystalline HA phase, as shown in the curve labeled (c-f) in Fig. 3.

The calculated amounts of crystallite size (*d*) of the hydroxyapatite powders which were synthesized different P_2O_5 dosages based on the diffraction peak and using Scherrer's equation are also listed in Table 2. The crystallite sizes of the hydroxyapatite powders with crystallites of 17-25 nm. An increase in crystallite size of the hydroxyapatite powders with increasing of P_2O_5 dosages was observed, i.e. the higher of the P_2O_5 dosages, the larger of the crystallite size of the hydroxyapatite powders.

The FTIR spectra of RWA: P_2O_5 used with the molar ratio 10:7 prepared hydroxyapatite powder which was sintered at 800 °C is shown in Fig. 4. In the spectra, bending and stretching modes of P–O vibrations are present as bands around 557, 962, 1033 and 1068 cm^{-1}, respectively [9,11]. The bands at 2852 and 2921 cm^{-1} are attributed to the asymmetric stretching of CH_2 and CH_3 [9]. The bands assigned to the stretching modes of hydroxyl groups (OH) in the hydroxyapatite (3571 cm^{-1} and 474 cm^{-1}) [11] can be clearly observed in the spectra. Additionally, the carbonate ion substitution is identified by characteristic peaks of the carbonate ions around 864 and 1434 cm^{-1}, which are attributed to the vibrational modes of the carbonate ions substituted at the phosphate sites (B-type). Moreover, the carbonate ion band at 1550 cm^{-1} can be ascribed to A-type carbonate substitution on hydroxide ion sites [9]. However, many different studies have resulted in contradictory explanations regarding which bands correspond to type A, type B or mixed type AB carbonate substitution [11]. In this experiment, the carbon peaks observed for the specimens the peak at 1465–1415 cm^{-1} and 1227 cm^{-1} [10-11]. The presence of the peak at 1465 cm^{-1} is related to CO_3^{2-} group and suggests that carbon from the organics does not pyrolyze completely and may instead dissolve into the hydroxyapatite crystal [11].

The presence of carbonate is a form of lattice defect in the HA, which could contribute to its low crystallinity, supporting the XRD data. The more the carbonated the powder is, the more the diffraction peaks broaden. It should be mentioned that most biological apatite contain both A- and B-type carbonate ions in their lattices. It can thereby be concluded that the prepared HA is chemically and structurally analogous to biological apatite. The apatite in natural bone contains significant amounts of carbonate ions, from about 4 to 6 wt%. In general, low carbonate content can improve the bioactivity of HA [9]. The SEM micrographs showed the morphology and particle size was spherical shapes. The HA formed using RWA was an assembly of uniform spherical-like nanoparticles. A close look shows that these agglomerates are made up of clusters of sphere. The average grain size of calcium phosphate powders found from SEM images is to be around 50–100 nm.

Table 1.Chemical compositions (%) with X-ray fluorescence analysis of RWA compared with commercial ($CaHPO_4$)

Samples	CaO	SiO_2	K_2O	MgO	P_2O_5	Al_2O_3	Fe_2O_3	SO_3	Cl	LOI[a](800°C)
RWA	49.76	1.52	8.44	3.50	1.86	0.26	0.26	1.28	0.30	32.82
[a]Total percentage of mass loss includes the organic material.										
Commercial ($CaHPO_4$), Calcium phosphate, assay 98-102.5% carbonate in accordance, chloride (Cl^-) ≤200 mg/kg, sulfate (SO_4^{2-})≤3000 mg/kg, Fe ≤3000 mg/kg 24.50-26.50% loss on ignition at 800°C										

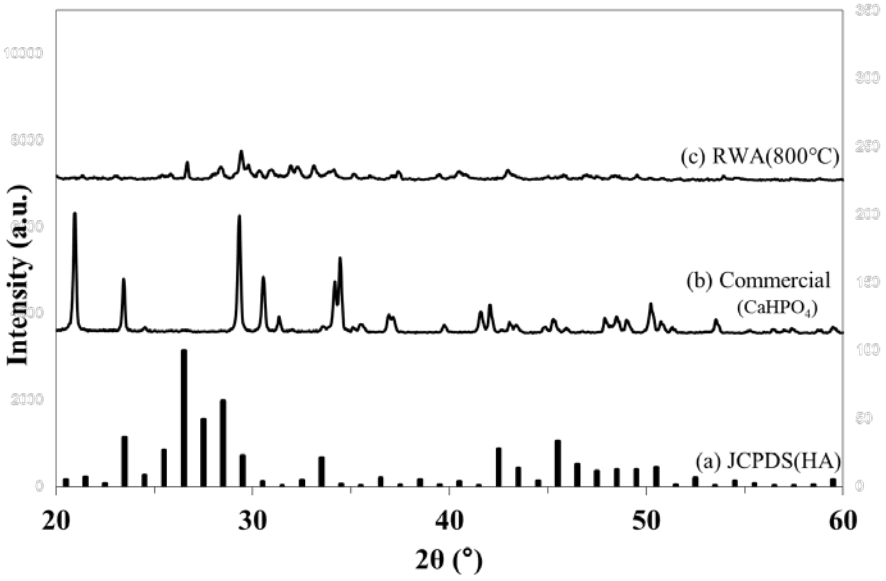

Fig. 2. XRD pattern of (a) hydroxyapatite (JCPDS 09-0432) (b)commercial ($CaHPO_4$) and (c) RWA sintered at 800°C

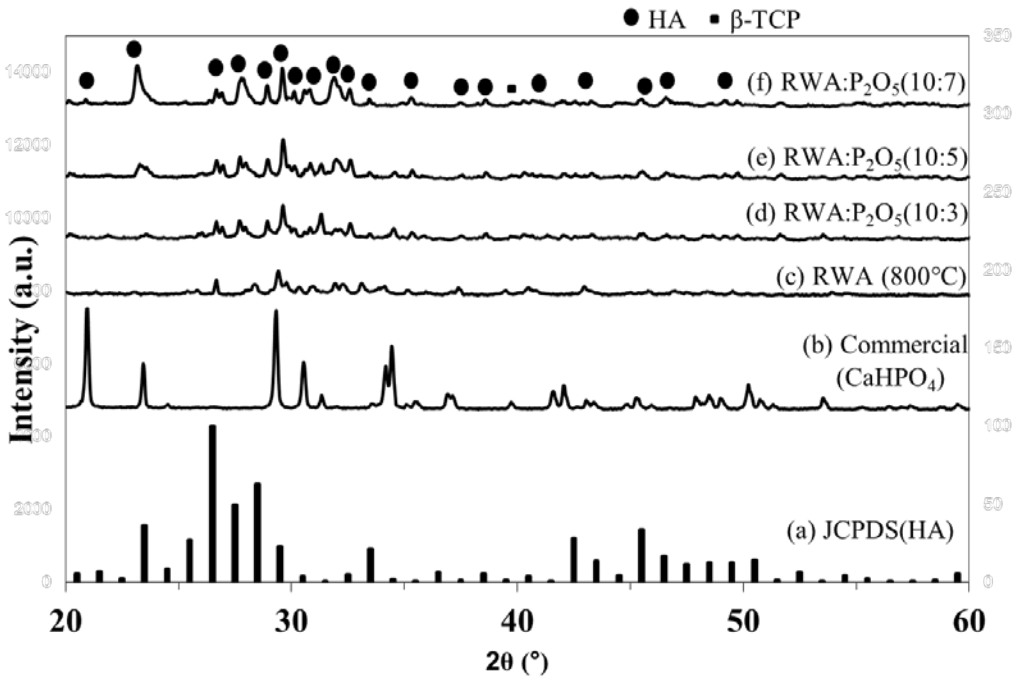

Fig. 3. XRD pattern of (a) hydroxyapatite (JCPDS 09-0432) (b) (c) RWA sintered at 800°C and RWA:P_2O_5 sintered at 800°C with the molar ratio (d) 10:3, (e) 10:5 and (f) 10:7

Table 2.The effect of P_2O_5on the crystallinity and crystallite size of prepared hydroxyapatite powders

Samples (RWA:P_2O_5)	Crystallinity,*Fc* (%)	Crystallite size, *d*(nm)
10:3	81	17
10:5	83	22
10:7	87	25

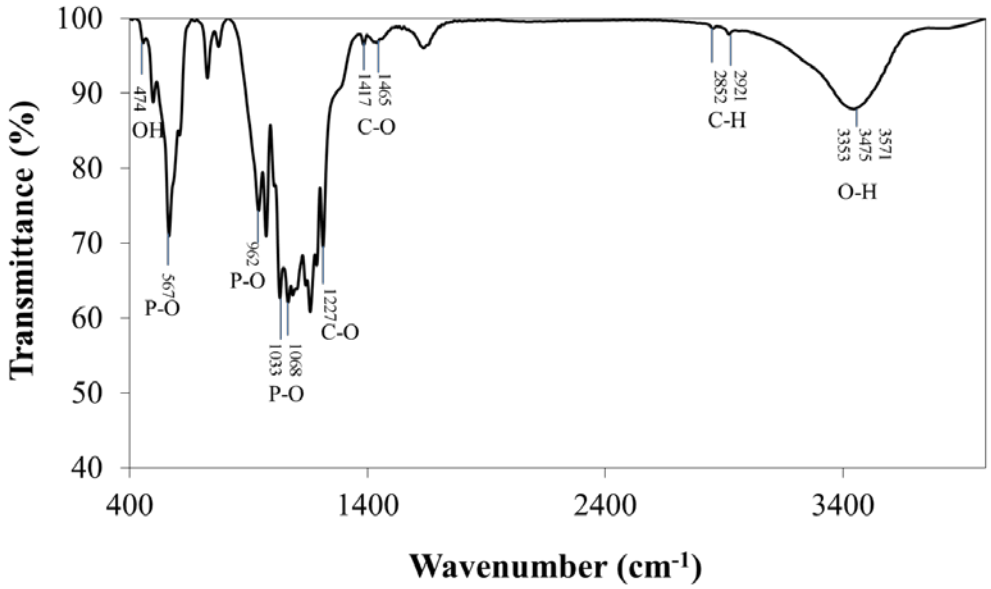

Fig. 4. The FTIR spectra of RWA:P_2O_5 used with the molar ratio 10:7 prepared hydroxyapatite powder sintered at 800 ˚C.

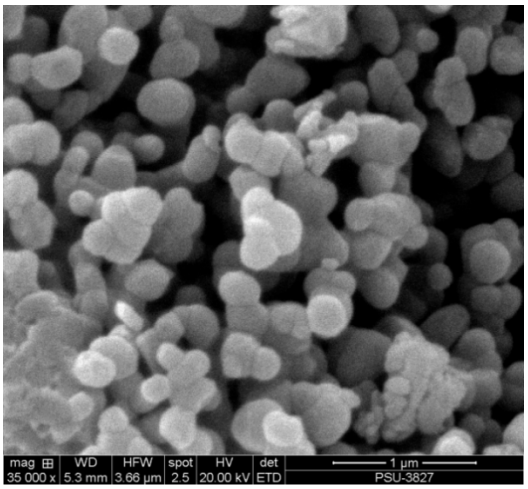

Fig.5. SEM images of synthesized calcium phosphate bioceramic powders of RWA:P_2O_5 at 10:7 sintered at 800°C at 35,000X.

4. Conclusions

It has been demonstrated that it is possible to use waste rubber wood ash as a calcium source to form lime (calcium oxide) and then hydroxyapatite (HA) by sintered at 800°C. The HA produced was comparable to a hydroxyapatite (JCPDS 09-0432), although the as-synthesized material contained residual phases β-TCP ($Ca_3(PO_4)_2$) due to incomplete calcination. This β-TCP was removed by the subsequent heat treatment step following HA production. The prepared HA powders at different amount of P_2O_5 dosages, results have shown that RWA: P_2O_5 at10:7 the hydroxyapatite Nano powder with crystallites of 17-25 nm size was prepared via a simple sol–gel method. Although rubber wood ash is a waste material, the present investigation shows that HA Nano crystalline can be successfully prepared by a simple method at room temperature from rubber wood ash.

Acknowledgments

This investigation was supported by faculty of engineering Rajamangala University of Technology Srivijaya, Songkhla, Thailand. The authors would like to thank Assoc. Prof. Dr. Lek Sikong, Lecturer and Mr. Panumart Choopool at the Prince of Songkla University, for their facility supports.

References

[1] F. Kusmanto, G.Walker, Q. Gan, P. Walsh, B. Fraser, and G. Dickson,"Development of Composite Tissue Scaffolds Containing Naturally Sourced Mircoporous Hydroxyapatite", Chemical Engineering Journal, Vol. 139, 2008, pp.398–407.

[2] M. Malmsten, "Inorganic Nanomaterials as Delivery Systems for Proteins, Peptides, DNA, and siRNA",Current Opinion in Colloid & Interface Science,Vol. 18, 2013, pp.468–480.

[3] M. Vallet-Regi, and JM. Gonzalez-Calbet, "Calcium Phosphates as Substitution of Bone Tissues", *Progress in Solid State Chemistry*, Vol. 32, 2004, pp. 1–31.

[4] MA. Rauschmann, TA. Wichelhaus, V. Stirnal, E. Dingeldein, L., Zichner, R., Schnettler, and V.,Alt, "Nanocrystalline Hydroxyapatite and Calcium Sulphate as Biodegradable Composite Carrier Material for Local Delivery of Antibiotics Inbone Infections", Biomaterials, Vol. 26, 2005, pp. 2677–2684.

[5] M. Zahouily, W. Bahlaouan, B. Bahlaouan, and A. Rayadh, "Catalysisby Hydroxyapatite Alone and Modified by Sodium Nitrate: a Simpleand Efficient Procedure for the Construction of Carbon-Nitrogen Bondsin Heterogeneous Catalysis", Arkivoc, Vol 13, 2005, pp. 150–161.

[6] T. Kawai, C. Ohtsuki, M. Kamitakahara, M. Tanihara, T. Miyazaki,Y. Sakaguchi, and S. Konagaya, "Removal of Formaldehyde by Hydroxyapatite Layer Biomimetically Deposited on Polyamide Film", Environmental Science & Technology, Vol. 40, 2006, pp.4281–4285.

[7] A. Jungbauer, R. Hahn, and K. Deinhofer, "Performance and Characterization of a NanophasedPorous Hydroxyapatite for Protein Chromatography", Biotechnology and Bioengineering, Vol. 87, 2004, pp. 364–375.

[8] WJ. Shih, YF. Chen, MC. Wang and MH. Hon, "Crystal Growth and Morphology of the Nano-sized Hydroxyl apatite Power Synthesized from $CaHPO_4$-$2H_2O$ and $CaCO_3$ by Hydrolysis Method", Journal of Crystal Growth, Vol. 270, 2004, pp. 211-18.

[9] W. Shih-Ching, T. Hsi-Kai, H. Hsueh-Chuan, H. Shih-Kuang, L.Shu-Ping, and H.Wen-Fu, "A Hydrothermal; Synthesis of Egg Shell and FRuit Waste Extract to Produce Nanosized Hydroxyapatite", Ceramics International , Vol. 39, 2013, pp. 8183–8188.

[10] M. Wojasiń Ski, E. Duszyńska, T. Ciach, "Lecithin-based Wet Chemical Precipitationof Hydroxyapatite Nanoparticles", Colloid and Polymer Science, Vol. 293, 2015, pp. 1561–1568.

[11] M.H. Fathi, A. Hanifi, and V. Mortazavi, "Preparation and Bioactivity Evaluation of Bone-like Hydroxyapatite Nanopowder" , Journal of Materials Processing Technology, Vol. 202, 2008, pp. 536–542.

[12] W. Shin-Ching, H. Hsueh-Chuan, W. Yu-Ning, H. Wen-Fu, "Hydroxyapatite synthesis from oyster shell powers by ball milling and heattreatment", Journal Materials Characterization, Vol 62, 2011, pp.1180-87.

[13] R. Sawittree, K. Pitoon, and W. Panthong,"Synthesis of Hydroxyapatite from Oyster Shell via Precipitation", EnergyProcedia, 56, 2014, pp. 112–117.

[14] M.R. Eric, A. Miguel, B. Witold, V.M. Castaño Victor, J.R. Dıaz-Estrada, R. Hernandez, and J. Rogelio Rodrıguez, "Synthesis of Hydroxyapatite from Eggshells", Materials Letters, Vol. 41, 1999, pp. 128–134.

[15] B.M. Jadwiga, H. Krzysztof, S. Maciej, M. B. Mirosław, and M. Beata, "Hydroxyapatite from Animal Bones–Extraction and Properties", Ceramics International, Vol. 41, 2015, pp. 4841–4846.

[16] H.S. Jun, I.J. Mark, and A.P. Darrell., "Greener Photocatalysts: Hydroxyapatite Derived from Wastemussel Shells for the Photocatalytic Degradation of a Modelazo Dye Wastewater", Chemical Engineering Research and Design, Vol. 91, 2013, pp. 1693–1704.

[17] P. Weeraphat, S. Panan, C. Narattaphol, T. Jirawan, K. Nateetip, and I. Ming Tang, "Hydroxyapatite from FIsh Scale for Potential Use as Bone Scaffold or Regenerative Material", Materials Science and Engineering C, Vol. 62, 2016, pp. 183–189.

[18] M. Masae, L. Sikong, P. Kongsong, P. Phoempoon, S. Rawangwong, and W. Sririkun, "Application of Rubber Wood Ash for Removal Nickel and Copper from Aqueous Solution", Environment and Natural Resources Journal, Vol. 11, 2013, pp. 17-27.

[19] Z. Liuxue, L. Peng, and S. Zhixing, "Photocatalysis Anatase Thin Film Coated. PAN Fibers Prepared at Low Temperature", Materials Chemistry and Physics, Vol. 98, 2006, pp. 111–115.

[20] E. Landi, A. Tampieri, G. Celotti, and S. Sprio, "Densification Behavior and Mechanisms of Synthetic Hydroxyapatites", Journal of the European Ceramic Society, Vol. 20, 2000, pp. 2377–2387.